

ADVANCEMENT OF THE CLOSELY COUPLED PROBES POTENTIAL DROP TECHNIQUE FOR NDE OF SURFACE CRACKS

F. Takeo¹ and M. Saka²

¹ Hachinohe National College of Technology, Hachinohe, Japan; ² Tohoku University, Sendai, Japan

Abstract: DCPD technique is powerful tool for quantitative NDE of cracks. The technique using four probes which are in close proximity to each other has been proposed for NDE of surface cracks; that is the closely coupled probes potential drop (CCPPD) technique. It has been shown that the sensitivity of the CCPPD technique is enhanced significantly in comparison with the usual method.

The objective of this study was to advance the CCPPD technique. An appropriate probes distance to enhance reproducibility was found by experiment. The d-c potential fields were analyzed for many cases of crack length $2a$, crack depth b and material thickness t by using FEM. By using the numerical results, the calibration equation which relate the potential drop to a , b , and t was obtained. Then the procedure to evaluate crack depth more accurately in two steps was proposed. Experiments validated the use of the technique for NDE of surface cracks.

Introduction: D-c potential drop technique is suitable for quantitative NDE of cracks. It has been applied not only to single crack but also multiple cracks [1].

The technique using four probes, which are in close proximity to each other, has been proposed [2][3]; that is the closely coupled probes potential drop (CCPPD) technique. It has been shown that the sensitivity of the CCPPD technique is enhanced significantly in comparison with the usual method using a uniform current flow in the region far from the crack. In addition, the CCPPD technique is suitable for fields which require smaller equipment and sensor being easy to deal with.

There are some cases where the reproducibility of potential drop measurement is required to be enhanced. An error in probes positioning is sometimes encountered in those cases. The potential abruptly increases as closing the current input-output probes because a current density takes higher value in the vicinity of these points. So a larger error may be introduced in the measured potential drop due to a small error in probe positioning. The purpose of this study is to enhance the reproducibility of evaluation of the crack depth on the surface by the CCPPD technique. At first, appropriate distance between probes to enhance reproducibility of measurement is found by experiment. Next, the potential drops for many cases of crack length $2a$, crack depth b and material thickness t are analyzed by using the appropriate probe distance by finite element method (FEM). By using the analyzed results, the calibration equation that approximately relates the potential drop with a , b and t is obtained. Then the method to evaluate crack depth with two steps is adopted. Through these two steps, more accurate b can be evaluated. The reproducibility of crack depth evaluation is ascertained by experiment.

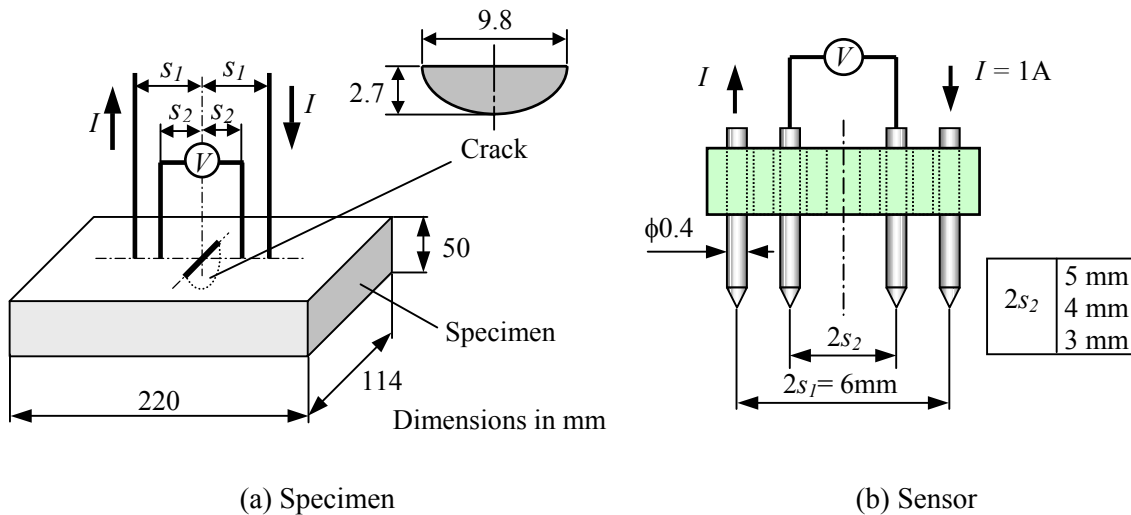


Fig.1 Schematic of experimental apparatus

Appropriate Distance between Probes: The appropriate distance between probes to enhance reproducibility of measurement was examined through an experiment. The specimen was made of austenitic stainless steel AISI304, and had the width 114mm, the length 220mm and the thickness 50mm as shown in Fig. 1(a). The crack was modeled by a semi-elliptical slit having the width 0.1mm, which was introduced by electric-discharge machining. The crack length was 9.8mm and the depth 2.7mm. Two probes for current input-output and two probes for measuring potential drops were located at $\pm s_1$ and $\pm s_2$ from the crack respectively, and on perpendicular bisector of the crack line as shown in Fig. 1(a). Constant d-c current in the amount of 1A was applied to the specimen through the current input and output probes. The potential drop V was measured between measuring probes. All four probes were synthesized to build a pen-like sensor. So the sensor is small and easy to deal with. The contact of every probe to the specimen surface was made constant by using springs. At the top of the sensor, there are some holes to insert probes as shown in Fig. 1(b). So the probe distances can easily be changed. In this experiment, the distance between current input-output probes $2s_1$ was made constant as 6mm, and the distance between measuring probes $2s_2$ was changed with 3, 4, and 5mm. The values of potential drop at uncracked part V_0 and that at cracked part V_1 were measured for 50 times respectively, and the effect of probe distance on the reproducibility of measurement was examined.

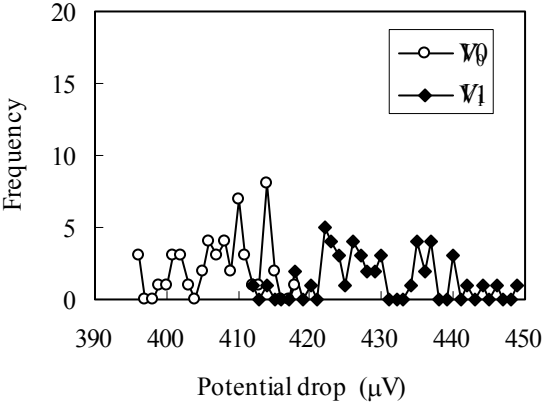


Fig. 2 Frequency distribution of the measured potential drop ($2s_2=5\text{mm}$)

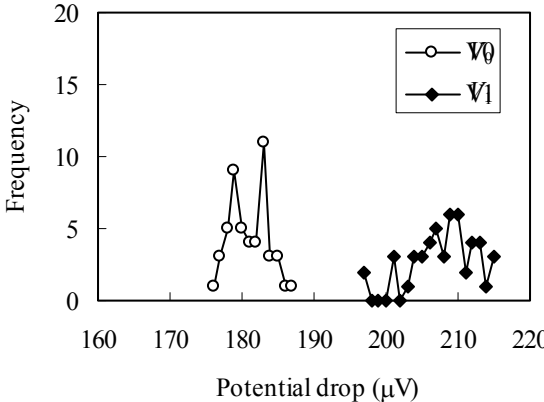


Fig. 3 Frequency distribution of the measured potential drop ($2s_2=4\text{mm}$)

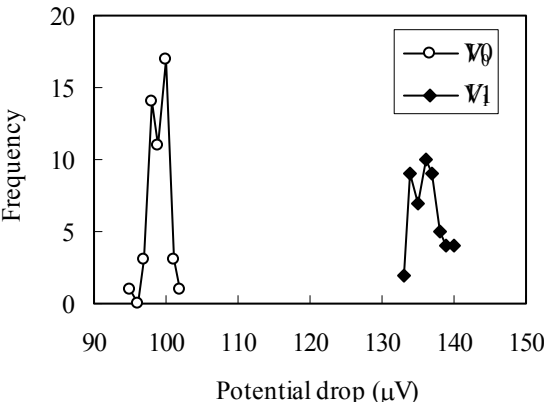


Fig. 4 Frequency distribution of the measured potential drop ($2s_2=3\text{mm}$)

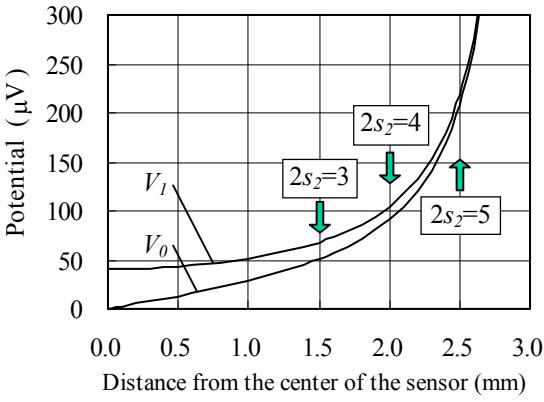


Fig. 5 Distribution of the potential

Figures 2, 3 and 4 show the frequency distribution of measured potential drops. The potential drop V_0 and V_1 become large as s_2 . There are some variations in all cases. The range of variation for the case of $2s_2 = 5\text{mm}$ is larger than that for the case of $2s_2 = 3\text{mm}$. As one of the reason for this, it may be possible to consider that the probes distances contain a slight error caused by clearance between probe and inserted hole. Figure 5 shows the distribution of potential in the half region between current input-output probes. Potential in Fig. 5 was calculated by using FEM for the case of resistivity of materials $\rho = 72 \times 10^{-8} \Omega\text{m}$. The positions of measuring probe for the cases of $2s_2 = 3, 4$ and 5mm are shown in Fig. 5. It was found that potential abruptly increases as close to current input-output probe. When measuring probes are located in this region, a larger error may be introduced in the measured potential drop from a slight error in probes positioning. For the case of $2s_2 = 3\text{mm}$, measuring probe is located at the position where the distribution of potential is not so steep and rather large value of voltage can be measured. And also the big change in potential drop can be obtained by crack. Then $2s_2 = 3\text{mm}$ is decided to be a suitable probe distance to enhance reproducibility of measurement for $2s_1 = 6\text{mm}$.

Calibration Equation: Let us consider the way to evaluate a crack depth by using the probe distance $2s_1 = 6\text{mm}$ and $2s_2 = 3\text{mm}$ that obtained from the previous discussion. In this study, only an open crack on the surface was considered. Then crack length $2a$ and material thickness t can be measured, and only crack depth b is unknown. The ranges of crack size and material thickness treated in this study are as follows:

$$1.0\text{mm} \leq t \leq 20\text{mm} \text{ and } t = \infty$$

$$0.5\text{mm} \leq a \leq 20\text{mm} \text{ and } a = \infty$$

$$0.5\text{mm} \leq b \leq 20\text{mm} \text{ (only the range } b \leq a \text{ and } b < t)$$

At first, the relations between potential drop and crack size for many cases were calculated. The problem of d-current flow in a material is governed by the Laplace equation as

$$\nabla^2 \phi = 0 \tag{1}$$

where ϕ is the electrical potential and ∇^2 is the three-dimensional Laplace operator. Equation (1) can easily be solved by using FEM. The potential drops for various combinations of a , b and t were analyzed by FEM.

Next, the relations between potential drop and a , b and t were approximated with the following calibration equation [3]:

$$V_1 = \left\{ F\left(\frac{b}{s_2}\right) D\left(\frac{a}{s_2}, \frac{b}{a}\right) + 1 \right\} \times C(a, b, s_2, t) \times V_0 \tag{2}$$

where

$$F\left(\frac{b}{s_2}\right) = \ln \left[\frac{\ln \left\{ \left(\alpha \frac{b}{s_2} \right)^\beta + 1 \right\}}{\gamma} + 1 \right] \times \xi \tag{3}$$

$$D\left(\frac{a}{s_2}, \frac{b}{a}\right) = \exp \left[-\delta \left(\frac{a}{s_2} \right)^{-\zeta} \left(\frac{b}{a} \right)^{\left\{ \eta \left(\frac{a}{s_2} \right) + \phi \right\}} \right] \tag{4}$$

$$C(a,b,s_2,t) = \begin{cases} \left(\lambda \frac{s_2}{t} \right)^\kappa \frac{a}{s_2} \left(\frac{b}{t} \right)^3 + 1 & \text{(for } a \leq 20\text{mm)} \\ \theta \left(\frac{s_2}{t} \right)^\zeta \frac{b}{t-b} + 1 & \text{(for } a = \infty) \end{cases} \quad (5a)$$

$$C(a,b,s_2,t) = \begin{cases} \left(\lambda \frac{s_2}{t} \right)^\kappa \frac{a}{s_2} \left(\frac{b}{t} \right)^3 + 1 & \text{(for } a \leq 20\text{mm)} \\ \theta \left(\frac{s_2}{t} \right)^\zeta \frac{b}{t-b} + 1 & \text{(for } a = \infty) \end{cases} \quad (5b)$$

and V_0 is the potential drop in an uncracked part.

Coefficients of Eqs. (3) to (5) were obtained for the following four cases:

Case 1: $a \leq 20\text{mm}$, $t = \infty$

Case 2: $a \leq 20\text{mm}$, $t \leq 20\text{mm}$

Case 3: $a = \infty$, $t = \infty$

Case 4: $a = \infty$, $t \leq 20\text{mm}$

Table 1 Coefficients of the calibration equation

Cases	Case 1					Case 2			
	a	$a \leq 20 \text{ mm}$							
	t	$t = \infty$				$t \leq 20 \text{ mm}$			
	b	1st step	2nd step			1st step	2nd step		
		$b \leq 1.5$	$b \geq 10$	$1.5 < b < 10$		$b \leq 2$	$b \geq 12$	$2 < b < 12$	
Coefficients	α	0.203	0.06391	0.1853	0.2795	0.203	0.06391	0.1853	0.2795
	β	2.95	2.019	2.646	2.518	2.95	2.019	2.646	2.518
	γ	0.0025	0.003464	0.001376	0.02088	0.0025	0.003464	0.001376	0.02088
	ξ	0.126	0.2547	0.12	0.1779	0.126	0.2547	0.12	0.1779
	δ	0.8	0.7246	0.8148	0.7885	0.8	0.7246	0.8148	0.7885
	ζ	1.23	0.8826	1.2	1.185	1.23	0.8826	1.2	1.185
	η	0.15	0.236	0.04209	0.07574	0.15	0.236	0.04209	0.07574
	φ	0.32	0.2758	0.6729	0.5476	0.32	0.2758	0.6729	0.5476
	λ					0.186	0.0005393	0.7509	0.2337
	κ					1.31	0.3226	2.202	1.436

Cases	Case 3					Case 4			
	a	$a = \infty$							
	t	$t = \infty$				$t \leq 20 \text{ mm}$			
	b	1st step	2nd step			1st step	2nd step		
		$b \leq 2$	$b \geq 10$	$2 < b < 10$		$b \leq 2$	$b \geq 12$	$2 < b < 12$	
Coefficients	α	0.185	0.05296	0.1591	0.2879	0.185	0.05296	0.1591	0.2879
	β	3.07	2.045	2.293	2.442	3.07	2.045	2.293	2.442
	γ	0.001295	0.001977	0.001824	0.02663	0.001295	0.001977	0.001824	0.02663
	ξ	0.118	0.2386	0.1315	0.1886	0.118	0.2386	0.1315	0.1886
	θ					0.0613	0.05124	0.1867	0.1313
	χ					0.897	0.3017	1.491	1.298

The calibration equation which was obtained for the all range of b , $0.5\text{mm} \leq b \leq 20\text{mm}$, would contain the regions where the accuracy of approximation is not enough. Then the evaluation procedure with two steps was adopted in this study. In the first step, an approximate value of b was evaluated by using the calibration equation for the all range of b . In the second step, calibration equation obtained for narrow range of b was selected based on the evaluated value of b in the first step. At last, the precise value of b was evaluated through the selected calibration equation. The coefficients of the equation obtained are shown in Table 1.

Results and Discussions: Figure 6 shows an example of the relationship between V_1/V_0 and b . Plotted marks and lines show the numerical results of FEM and calibration equation, respectively. The calibration equation shown in Fig. 6 is for the range of $b \geq 10\text{mm}$. It can be ascertained that the equation approximates the potential drop in that range. From Fig. 6, it can be found that the gradient of the calibration equation becomes smaller as crack depth becomes larger. This means the sensitivity decreases with increasing crack depth. So the adequate range of crack depth to evaluate sensitively seems to be $b \leq 5\text{mm}$ for the sensor with $2s_1 = 6\text{mm}$ and $2s_2 = 3\text{mm}$.

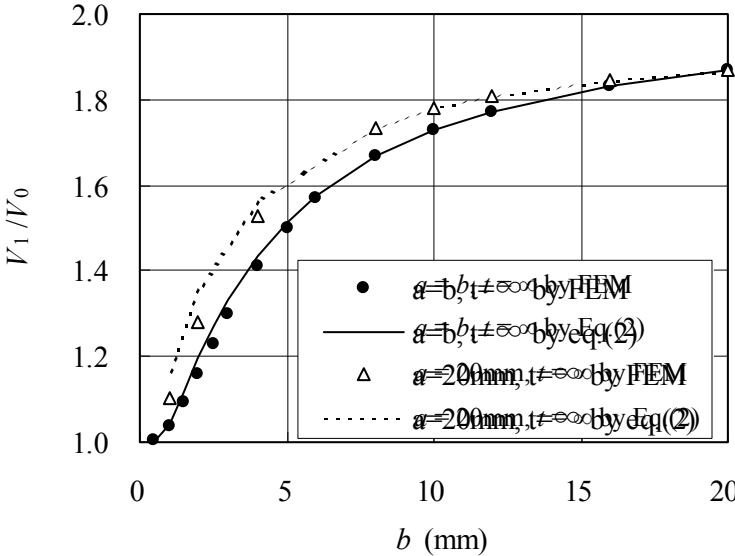


Fig.6 Example of the relationship between V_1/V_0 and b

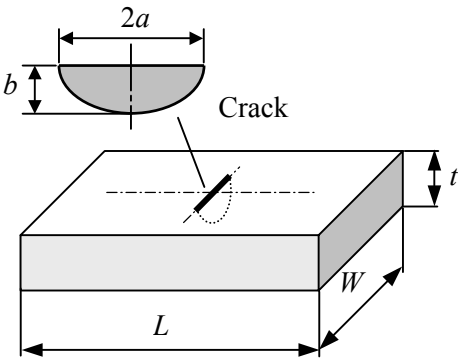


Fig.7 Shape of the specimen

Table 2 Size of the specimen

Specimen No.	101-L	306
Material	AISI304	
W (mm)	50	150
L (mm)	340	250
t (mm)	14.98	49.90
$2a$ (mm)	14.00	11.90
b (mm)	2.69	2.06

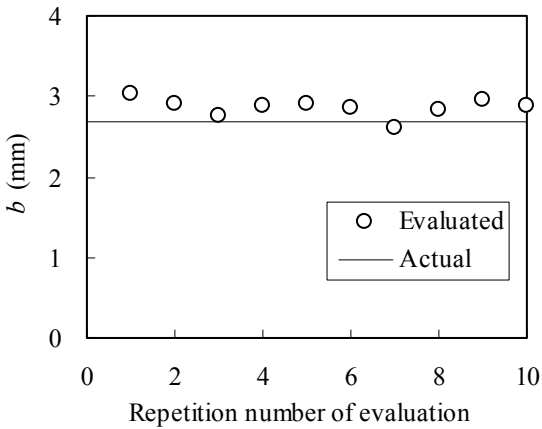


Fig.8 Example of evaluated result (No. 101-L)

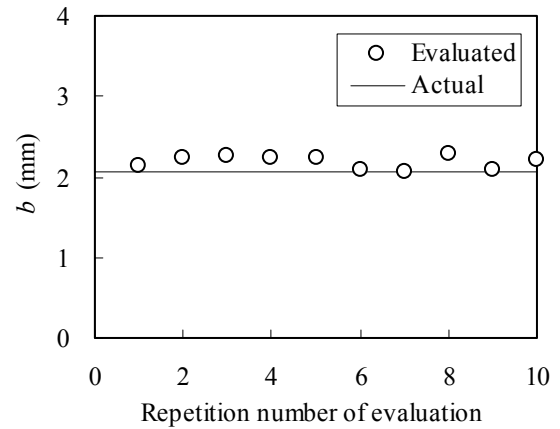


Fig.9 Example of evaluated result (No. 306)

The validity of the technique proposed in this paper was verified by experiment. The specimens were made of austenitic stainless steel AISI304, and their width W , length L , thickness t , crack length $2a$ and crack depth b are shown in Fig. 7 and Table 2. The crack was modeled by a semi-elliptical slit having the width 0.1mm, which was introduced by electric-discharge machining. Figures 8 and 9 show the evaluated depth which was measured continuously 10 times by hand. Lines in Figs. 8 and 9 show the actual depth of crack. There was a tendency to evaluate slightly deeper than the actual depth in both cases. The result generally shows good reproducibility of this technique.

Conclusions: In order to enhance the reproducibility of evaluation of the crack depth on the surface by the CCPD technique, appropriate distance between probes was found by experiment. The calibration equation that approximately relates the potential drop with a , b and t was obtained based on FEM. The procedure to evaluate crack depth with two steps was adopted to enhance the accuracy of evaluation. The reproducibility of crack depth evaluation is ascertained by experiment.

References:

- [1] H. Liu, M. Saka, H. Abé, I. Komura and H. Sakamoto, Trans. ASME, J. Applied Mechanics, Vol. **66**, 468 (1999).
- [2] M. Saka, A. Oouchi and H. Abé, Trans. ASME, J. Pressure Vessel Technology, Vol. **118**, 198 (1996).
- [3] M. Saka, D. Hirota, H. Abé and I. Komura, Trans. ASME, J. Pressure Vessel Technology, Vol. **120**, 374 (1998).